The Differential Roles of HSP90 Isoforms in Skin Inflammation: Anti-Inflammatory Potential of TRAP1 Inhibition

Hakim Ben Abdallah[1], Lars Iversen[1,2] and Claus Johansen[1]

Journal of Investigative Dermatology (2025) ■, ■–■; doi:10.1016/j.jid.2025.02.006

HSP90, a molecular chaperone, has been identified as a drug target in inflammatory skin diseases. However, 4 different HSP90 isoforms (HSP90α, HSP90β, GRP94, and TRAP1) exist. Therefore, this study aimed to evaluate the functional role of the HSP90 isoforms in skin inflammation. Selective knockdown of the HSP90 isoforms revealed different inflammatory effects in stimulated keratinocytes. TRAP1 knockdown significantly downregulated the expression of the measured inflammatory genes (*IL1B*, *IL6*, *IL17C*, *IL23A*, *IL19*, *IL36G*, *CXCL8*, *CCL5*, *CCL17*, *CCL20*). Selective and combined knockdown of HSP90α and HSP90β showed a trend toward increased inflammatory activity. Selective GRP94 knockdown and combined knockdown of the organelle-specific isoforms (GRP94 + TRAP1) or all 4 isoforms resulted in inconsistent effects. In addition, a selective TRAP1 inhibitor (gamitrinib) suppressed the inflammatory gene expression in keratinocytes and fibroblasts (*IL17C*, *IL23A*, *IL36G*) and in hidradenitis suppurativa skin cultured ex vivo (*IL1B*, *IL6*, *CXCL8*, *IL17A*, *IL36G*). In conclusion, selective and simultaneous knockdown of the HSP90 isoforms mediated different inflammatory effects, revealing that the HSP90 isoforms have distinct roles in skin inflammation. In addition, we discovered that inhibition of TRAP1 exerted consistent anti-inflammatory effects, suggesting that TRAP1 inhibitors may represent a topical therapeutic strategy for inflammatory skin diseases.

Keywords: Hidradenitis suppurativa, HSP90, Paralog, Psoriasis

INTRODUCTION

HSP90 is an important chaperone that folds and regulates the function of endogenous proteins (referred to as client proteins) (McClellan et al, 2005; Taipale et al, 2010). In humans, the HSP90 family include 4 isoforms located at different subcellular compartments: HSP90α (*HSP90AA1*) and HSP90β (*HSP90AB1*) in the cytoplasm, GRP94 (Gp96 or endoplasmin) (*HSP90B1*) in the endoplasmic reticulum, and TRAP1 (*TRAP1*) in the mitochondria (Biebl and Buchner, 2019; Maiti and Picard, 2022). Although the isoforms share similarities, they exhibit notable differences in structure, expression, and function (Ausili, 2023).

Hundreds of HSP90 client proteins with diverse functions have been identified, and inhibition of HSP90 may lead to the degradation of these client proteins (Echeverría et al, 2011; Picard, 2023). Given that several client proteins play essential roles in tumor proliferation and survival, HSP90 has been identified as a potential drug target for cancer (Miyata et al, 2013; Trepel et al, 2010). To date, approximately 20 HSP90 inhibitors (almost all pan-HSP90 inhibitors) have been evaluated as potential cancer treatments. However, their clinical development has been limited owing to unsatisfactory efficacy and prevalent adverse effects (Li and Luo, 2023; Yu et al, 2022). Recently, the development of isoform-selective HSP90 inhibitors has gained more attention, leading to the first approval of a HSP90 inhibitor (TAS-116, a selective HSP90α and HSP90β inhibitor) in 2022 for gastrointestinal stromal tumors in Japan (Hoy, 2022).

HSP90 has also attracted attention as a drug target in inflammatory skin diseases owing to the degradation of client proteins involved in proinflammatory signaling. These client proteins include ACT1 (a key adapter protein involved in IL-17 signaling), pattern-recognition receptors (eg, toll-like receptors), signaling kinases (eg, Jaks and MAPKs), and transcription factors (eg, signal transducer and activator of transcriptions and NF-κB) (Costa et al, 2020; Wang et al, 2013). Recently, 2 proof-of-concept studies demonstrated that RGRN-305 (a pan-HSP90 inhibitor with preferential inhibition of HSP90α and HSP90β) resulted in a meaningful clinical efficacy with a good tolerability and safety profile in patients with psoriasis or hidradenitis suppurativa (Ben Abdallah et al, 2024; Bregnhøj et al, 2022). Moreover, pan-HS90 inhibitors (RGRN-305, tanespimycin, alvespimycin) have also been demonstrated to reduce skin inflammation in animal models of atopic dermatitis, psoriasis, irritant contact dermatitis, and epidermolysis bullosa acquisita (Ben Abdallah et al, 2023a, 2023b; Stenderup et al, 2014; Tukaj et al, 2017, 2014). These studies demonstrated that HSP90

[1]Department of Dermatology and Venereology, Aarhus University Hospital, Aarhus, Denmark; and [2]MC2 Therapeutics A/S, Hørsholm, Denmark

Correspondence: Hakim Ben Abdallah, Department of Dermatology and Venereology, Aarhus University Hospital, Palle Juul-Jensens Boulevard 45, 8200 Aarhus, Denmark. E-mail: hba@clin.au.dk

Abbreviation: siRNA, small interfering RNA

Received 9 September 2024; revised 3 February 2025; accepted 4 February 2025; accepted manuscript published online XXX; corrected proof published online XXX

inhibition exerted broad immunomodulation by downregulating numerous pivotal inflammatory signaling pathways, supporting the significance of HSP90 as an important regulator of numerous inflammatory client proteins.

Although these findings suggest that HSP90 may be a drug target for inflammatory skin diseases, the role of each isoform in inflammatory skin diseases has not been explored, which may provide insights that can be translated into potential therapeutic benefits.

Therefore, this study aimed to investigate the anti-inflammatory effects of selective inactivation of the HSP90 isoforms in chronic inflammatory skin diseases using experimental models with primary human keratinocytes and cultured human skin biopsies.

RESULTS

HSP90AA1, *HSP90AB1*, and *HSP90B1* were abundantly expressed among all cell types in the skin, whereas *TRAP1* was predominantly expressed in keratinocytes

An integrative analysis of publicly available single-cell RNA-sequencing datasets was performed to explore the gene expression of the 4 HSP90 isoforms—*HSP90AA1* (HSP90α), *HSP90AB1* (HSP90β), *HSP90B1* (GRP94), and *TRAP1* (TRAP1)—in cells from psoriasis (57,116 cells; n = 5), hidradenitis suppurativa (37,342 cells; n = 9), atopic dermatitis (46,922 cells; n = 5), and healthy (17,903 cells; n = 4) skin. The cell clustering identified 22 clusters that were annotated using signature genes as 11 cell types, including keratinocytes, fibroblasts, T cells, B cells, plasma cells, myeloid cells, vascular endothelial cells, lymphatic endothelial cells, melanocytes, smooth muscle cells, and mast cells (Figure 1a and b).

The 3 HSP90 isoforms *HSP90AA1*, *HSP90AB1*, and *HSP90B1* were ubiquitously and abundantly expressed among all cell types, whereas *TRAP1* was relatively lowly expressed and showed highest expression in keratinocytes (Figure 1c and d). The gene expression of the HSP90 isoforms in the different cell types varied among psoriasis, hidradenitis suppurativa, atopic dermatitis, and healthy skin (Figure 1e), indicating that the HSP90 isoforms may have different roles in skin diseases. Notably, *HSP90B1* was highly expressed in plasma cells from hidradenitis suppurativa skin, and *TRAP1* was expressed in a higher percentage of keratinocytes from psoriasis and hidradenitis suppurativa skin. To further validate the expression of TRAP1 in these inflammatory skin diseases, RT-qPCR demonstrated that *TRAP1* was moderately expressed with Ct values of approximately 30 (Supplementary Figure S1a). In addition, immunohistochemistry staining confirmed that TRAP1 was predominantly expressed in keratinocytes within the epidermis (Supplementary Figure S1b and c).

Taken together, these data indicate that HSP90α, HSP90β, and GRP94 serve different functions in all cell types in the skin, whereas TRAP1 may predominantly play a role in keratinocytes.

Selective knockdown of the HSP90 isoforms provided different effects on the expression of inflammatory genes in psoriasis-like stimulated keratinocytes

To examine the anti-inflammatory effects of the HSP90 isoforms, primary human keratinocytes from 6 healthy donors were transfected with small interfering RNA (siRNA) to knockdown the 4 different isoforms followed by a 'psoriasis-like' stimulation with TNF and IL-17A. The knockdown of the 4 different isoforms was efficient and specific with approximately 90−95% reduction of mRNA levels (Supplementary Figure S2) and 55−80% reduction of protein levels (Supplementary Figure S3). Moreover, inhibition of cytosolic HSP90 (ie, HSP90α/β) compared with that of GRP94 or TRAP1 may induce a more pronounced heat shock response with increased *HSP1A1* (HSP70) expression (Jiang et al, 2018; Park et al, 2020). This was consistent with our findings, further confirming the selective knockdown (Supplementary Figure S4a). The gene expression of key inflammatory genes was measured with qPCR, showing that the stimulation significantly upregulated the expression of *IL17C*, *IL23A*, *IL36G*, *IL19*, *CCL20*, *CXCL1*, and *NFKBIZ* (Figure 2). Interestingly, knockdown of the different HSP90 isoforms resulted in different effects on the inflammatory gene expression. Knockdown of *TRAP1* (ie, TRAP1 protein) led to significant downregulation of *IL17C*, *IL23A*, *IL36G*, *IL19*, and *CCL20* and trends of downregulation in *CXCL1* and *NFKBIZ*. Knockdown of *HSP90B1* (ie, GRP94 protein) led to significant downregulation of *IL36G*, *IL23A*, and *IL19*. Surprisingly, knockdown of the widely studied cytosolic isoforms, *HSP90AA1* or *HSP90AB1* (ie, HSP90α/β proteins), did not markedly reduce the inflammatory gene expression; in contrast, *HSP90AA1* knockdown increased the inflammatory gene expression (Figure 2). These findings suggest that selective knockdown of the HSP90 isoforms provides different inflammatory effects, and inhibition of TRAP1 may provide anti-inflammatory effects in keratinocytes.

Combined knockdown of the cytosolic HSP90 isoforms increased the inflammatory gene expression in psoriasis-like stimulated keratinocytes

Next, we explored the effects of combined knockdown on the cytosolic isoforms (*HSP90AA1* and *HSP90AB1*), the organelle-specific isoforms (*HSP90B1* and *TRAP1*), and all 4 isoforms (Supplementary Figure S5). Combined *HSP90AA1* and *HSP90AB1* knockdown increased the inflammatory gene expression (*IL17C*, *CXCL1*, *CCL20*), whereas knockdown of *HSP90B1* + *TRAP1* or all the isoforms decreased the expression of *IL36G* and *IL23A* but increased the expression of *CCL20* (Figure 3). Although selective TRAP1 inhibition consistently decreased the inflammatory gene expression of all measured genes, pan-inhibition of all isoforms downregulated only 2 of the measured inflammatory genes. These findings indicate that inhibition of TRAP1 drives the anti-inflammatory effects, whereas inhibition of the cytosolic isoforms (HSP90α/β) may induce proinflammatory gene expression in psoriasis-like stimulated keratinocytes.

To confirm the effects on protein levels, the protein expression of IL-17C and IL-36G was measured with ELISA and western blot, respectively. The measured protein levels were consistent with the gene expression findings (Figure 4), confirming that selective inactivation of the isoforms provides different effects. *TRAP1* knockdown significantly decreased the protein expression of IL-17C and IL-36G, whereas knockdown of the cytosolic isoforms had no effect or slightly increased the protein expression of IL-17C and IL-36G.

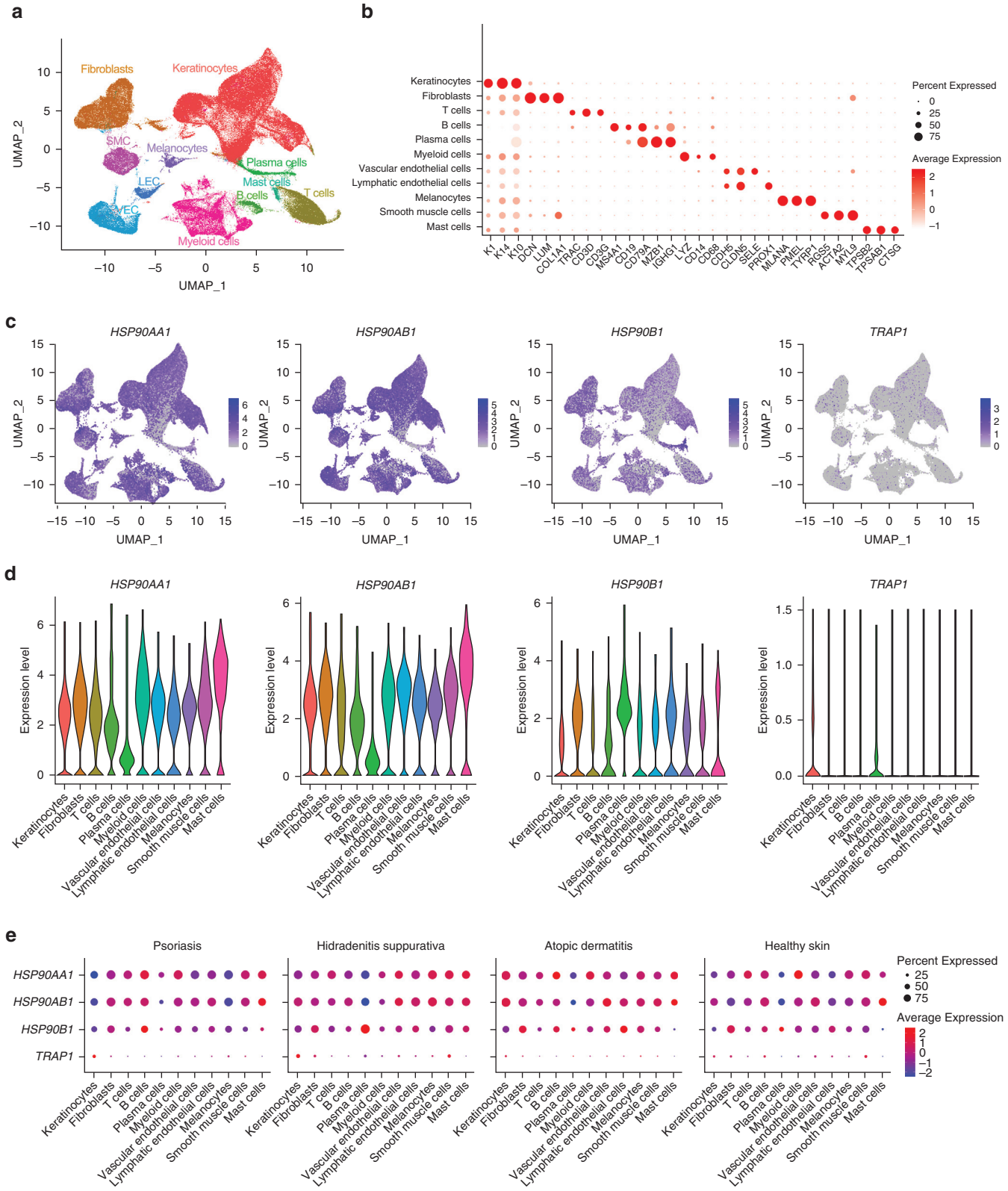

Figure 1. Integrative single-cell RNA sequencing analysis of the HSP90 isoforms in psoriasis, hidradenitis suppurativa, atopic dermatitis and healthy skin. (**a**) UMAP plot showing 159,283 cells coloured by cell type. (**b**) Dot plot showing the expression of marker genes used to annotate the cell types. (**c**) Feature plots and (**d**) violin plots depicting the expression levels of the four HSP90 isoforms among the cell types. Note: the y-axis range was set between 0 and 1.5 for the *TRAP1* violin plot (**e**) Dot plot of the HSP90 isoforms showing the differences among skin conditions and cell types. The colour scale depicts the average expression of the genes, whereas the dot size represents the percentage of cells expressing the gene of interest. K, keratin; LEC, lymphatic endothelial cell; SMC, smooth muscle cell; UMAP, Uniform Manifold Approximation and Projection; VEC, vascular endothelial cell.

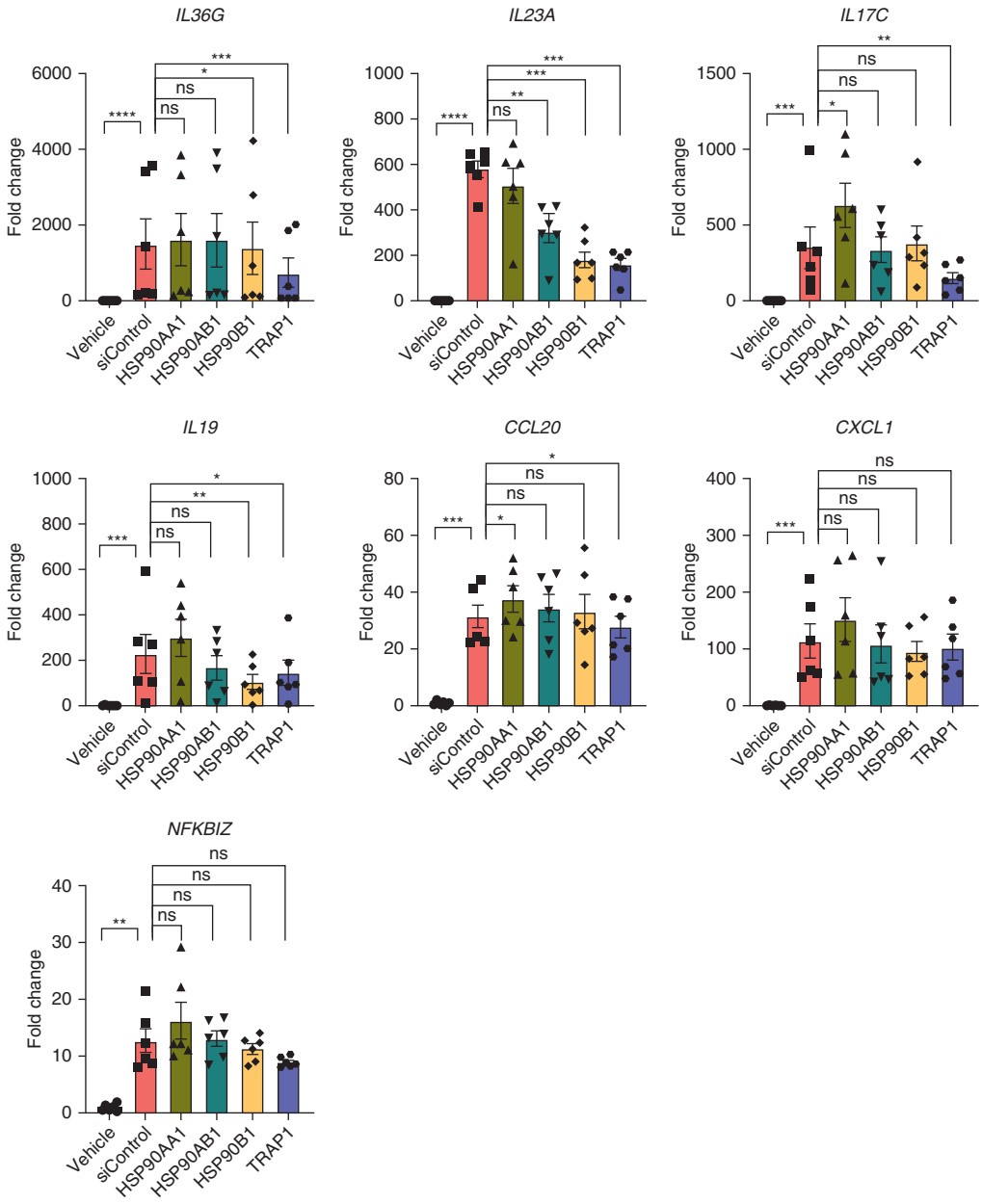

Figure 2. Effects of selective knockdown of the HSP90 isoforms in keratinocytes. Selective HSP90 isoform knockdown with siRNA was performed in primary human keratinocytes followed by stimulation with TNF (10 ng/ml) and IL-17A (100 ng/ml) for 24 hours (3 independent experiments, n = 6). Gene expression of the indicated inflammatory markers was measured with RT-qPCR and shown as mean (+SEM) fold change relative to the vehicle group. *P*-values were calculated by paired ratio *t*-tests. $*P < .05$, $**P \leq .01$, $***P \leq .001$, and $****P \leq .0001$. ns, not significant; siControl, control-targeted small interfering RNA; siRNA, small interfering RNA.

TRAP1-selective inhibitor (gamitrinib) significantly downregulated the gene expression of *IL17C*, *IL23A*, and *IL36G* in primary human keratinocytes and fibroblasts

To further validate that inhibition of TRAP1 provides anti-inflammatory effects, primary human keratinocytes stimulated with TNF + IL-17A were treated with a selective TRAP1 inhibitor (gamitrinib). Treatment with gamitrinib resulted in a significantly lower expression of *HSP1A1* (HSP70) than of TAS-116 (a selective HSP90α/β inhibitor), supporting that gamitrinib preferentially inhibited TRAP1 (Supplementary Figure S4b). Because *TRAP1* knockdown led to marked downregulation of *IL36G*, *IL23A*, and *IL17C* (Figure 2), the expression of these 3 cytokines were evaluated. In accordance, gamitrinib downregulated the gene expression of *IL36G*, *IL23A*, and *IL17C* (Figure 5a) and the protein expression of IL-17C and IL-36G in a dose-dependent manner (Figure 5b and c). Despite the *IL23A* mRNA clearly present in the stimulated keratinocytes, IL-23 protein could not be detected with western blot or ELISA. These findings further support that TRAP1 may be a driver of inflammation in keratinocytes.

The effects of gamitrinib were also evaluated in fibroblasts, a cell type with regulatory functions in skin inflammation. Gamitrinib strongly downregulated *IL36G*, *IL23A*, and *IL17C* to levels similar to those for unstimulated fibroblasts (Figure 5d), suggesting that TRAP1 inhibition may exert anti-inflammatory effects in other cell types beyond keratinocytes.

Selective *TRAP1* knockdown reduced the expression of T helper 1– and T helper 2–related genes in atopic dermatitis–like stimulated keratinocytes

To evaluate the effects of HSP90 isoforms on atopic dermatitis–like stimulation, selective and combined

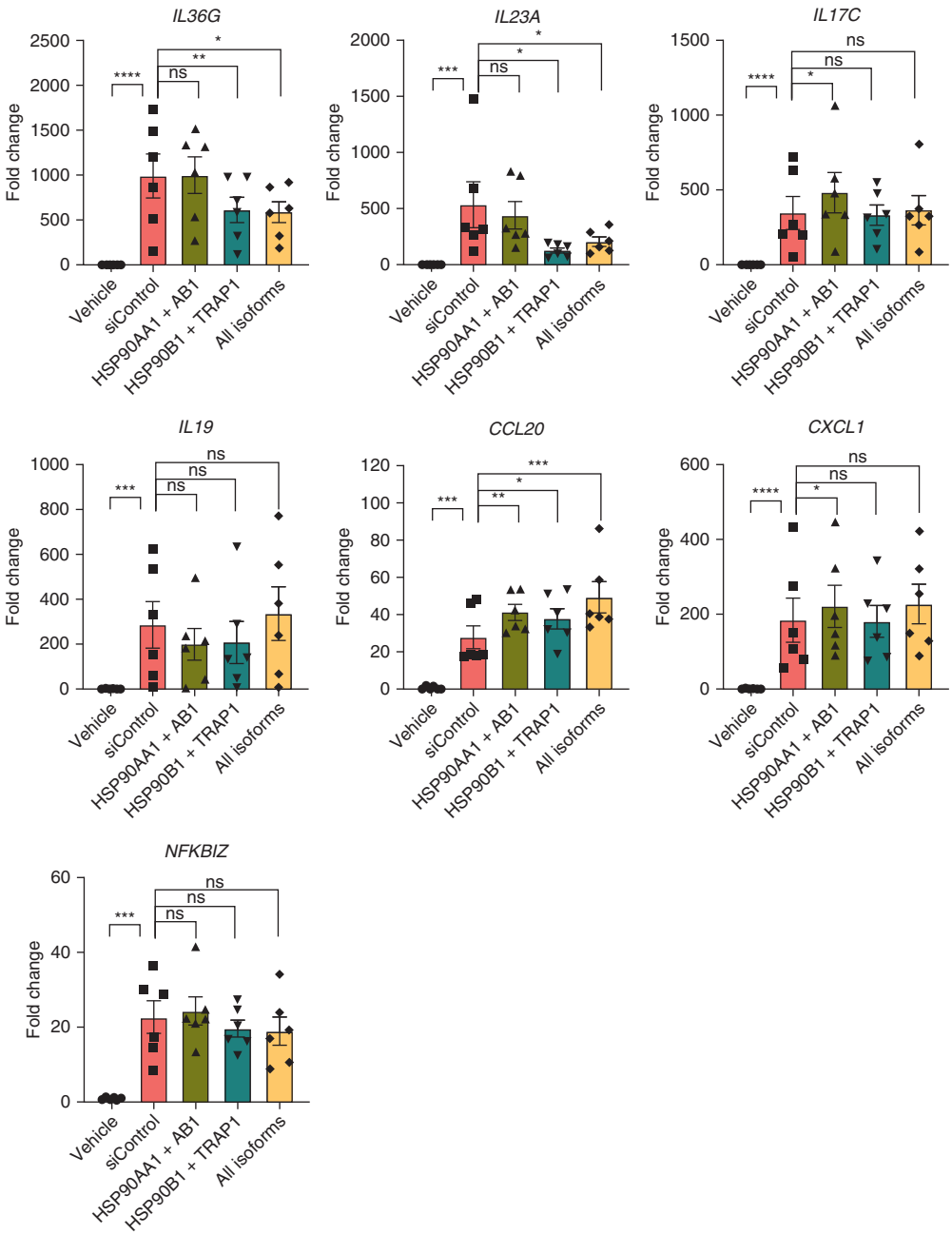

Figure 3. Effects of combined knockdown of the HSP90 isoforms in keratinocytes. Combined HSP90 isoform knockdown with siRNA was performed in primary human keratinocytes followed by stimulation with TNF (10 ng/ml) and IL-17A (100 ng/ml) for 24 hours (3 independent experiments, n = 6). RT-qPCR results of the indicated inflammatory markers are shown as mean (+SEM) fold change relative to the vehicle group. Wilcoxon rank-signed test was used for statistical analysis of *IL23A*, whereas paired ratio *t*-tests were used for the other comparisons. $*P < .05$, $**P \leq .01$, $***P \leq .001$, and $****P \leq .0001$. ns, not significant; siControl, control-targeted small interfering RNA; siRNA, small interfering RNA.

knockdowns of the HSP90 isoforms were performed in keratinocytes stimulated with TNF + IL-4 + IL-13. Interestingly, *TRAP1* knockdown significantly downregulated the expression of T helper 1–related (*IL1B*, *IL6*, *CXCL8*) and T helper 2–related (*CCL5*, *CCL17*) genes (Figure 6). Selective inactivation of *HSP90AA1*, *HSP90AB1*, or *HSP90B1* led to inconsistent effects on the measured genes, indicating no conclusive effect. Combined knockdown of the cytosolic isoforms (*HSP90AA1* + *HSP90AAB1*) significantly increased the inflammatory gene expression of *IL6*, *CXCL8*, and *CCL5*. Knockdown of the organelle-specific isoforms (*HSP90B1* + *TRAP1*) reduced the inflammatory gene expression; however, the reduction was not markedly greater than that of selective *TRAP1* knockdown, suggesting no additive anti-inflammatory effect of *HSP90B1* knockdown. Pan-inhibition of the HSP90 isoforms resulted in no significant effect besides increased expression of *IL6* and *CCL5*.

Consistent with the other results, inhibition of *TRAP1* provided anti-inflammatory effects, whereas inhibition of HSP90α/β induced proinflammatory gene expression in atopic dermatitis–like stimulated keratinocytes.

Gamitrinib suppressed the gene expression of inflammatory genes in lesional hidradenitis suppurativa skin cultured ex vivo

To evaluate the anti-inflammatory effects of TRAP1 inhibition in hidradenitis suppurativa, chronic lesional hidradenitis suppurativa skin from 14 patients was treated with gamitrinib in an ex vivo model. A total of 6 inflammatory markers

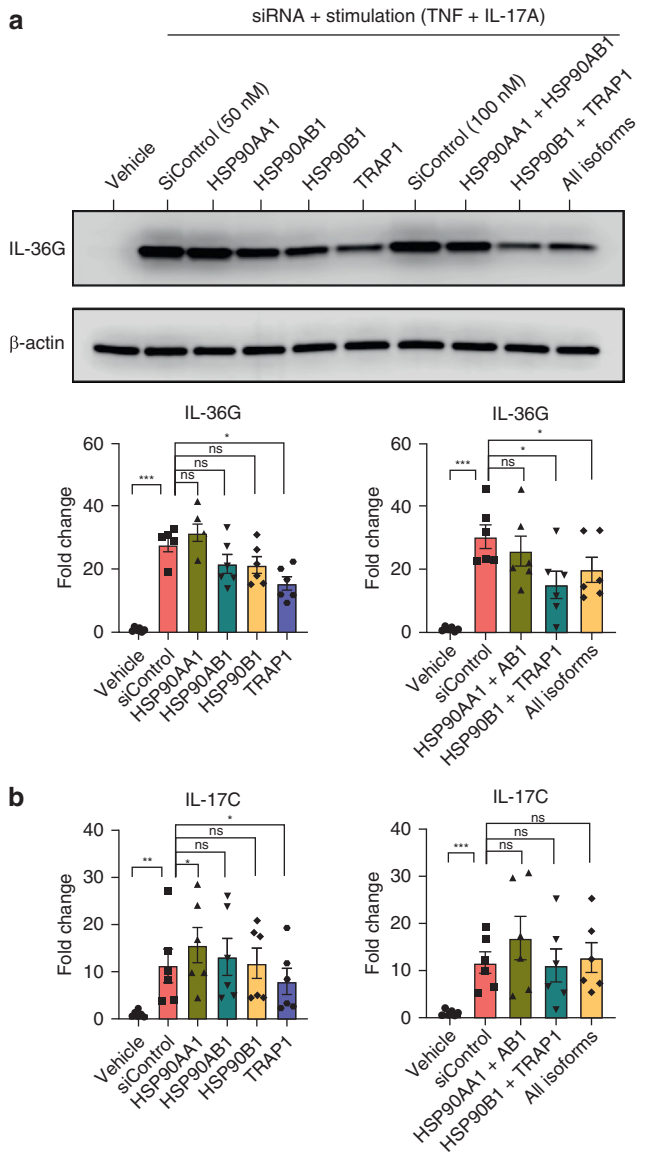

Figure 4. Effects of HSP90 isoform knockdown on the IL-36G and IL-17C protein expression in keratinocytes. The protein expression of IL-36G and IL-17C was determined in primary human keratinocytes transfected with the indicated siRNAs and stimulated with TNF (10 ng/ml) and IL-17A (100 ng/ml) for 24 hours. (**a**) Cell lysate protein expression of IL-36G was determined by western blot, showing representative western blots and the densitometric results. (**b**) Cell supernatant protein expression of IL-17C was determined by ELISA. Three independent experiments were performed (n = 6). Data are shown as mean (+SEM) fold change relative to the vehicle group. *P*-values were calculated by paired ratio *t*-tests. $*P < .05$, $**P \leq .01$, and $***P \leq .001$. ns, not significant; siControl, control-targeted small interfering RNA; siRNA, small interfering RNA.

associated with hidradenitis suppurativa were evaluated. Gamitrinib significantly downregulated the gene expression of *IL1B*, *IL6*, *CXCL8*, *IL17A*, and *IL36G*, whereas no effect was observed for *DEFB4A* (Figure 7). ELISA validated the downregulation of IL-1β and IL-6 at protein levels. The suppressive effects of gamitrinib were broadly similar to those of dexamethasone treatment. This supports that a preferential inhibition of TRAP1 may provide anti-inflammatory effects in hidradenitis suppurativa.

DISCUSSION

In this study, we demonstrated that selective and simultaneous knockdown of the HSP90 isoforms resulted in different inflammatory effects in keratinocytes, highlighting the distinct roles of HSP90α/β, GRP94, and TRAP1 in skin inflammation. In addition, we discovered that inhibition of TRAP1 provided strong anti-inflammatory effects, suggesting that TRAP1 may be a key driver for inflammation in keratinocytes. These findings indicate that the selectivity of HSP90 inhibitors toward specific isoforms may significantly influence their anti-inflammatory activity. This may have significant implications for the clinical development of HSP90 inhibitors in inflammatory skin diseases.

Although the literature is scarce, a few studies have examined the relationship between HSP90 isoforms and inflammation in diseases beyond dermatology. A recent study examined the anti-inflammatory effects of selective HSP90 isoform inhibitors in murine microglial BV-2 cells stimulated with lipopolysaccharide (Smith et al, 2024). The selective HSP90β inhibitor reduced the production of inflammatory mediators (*TNF*, *IL1B*, NF-κB, and extracellular signal–regulated kinase activation), whereas the selective Hsp90α, Grp94, TRAP1 inhibitors had limited anti-inflammatory effects (Smith et al, 2024). In agreement, siRNA-mediated knockdown of HSP90β but not HSP90α caused anti-inflammatory effects in N9 microglial cells (He et al, 2019). However, another study demonstrated that a selective HSP90β inhibitor, in contrast to HS90α/β inhibitors, failed to provide anti-inflammatory effects in lipopolysaccharide-stimulated bone marrow–derived macrophages, suggesting that the anti-inflammatory effects were mediated primarily by HS90α inhibition (Nizami et al, 2021). Moreover, a selective GRP94 inhibitor ameliorated inflammatory symptoms and protein expression of inflammatory markers (ie, TNF, IL-6, and p65) in a mouse model of ulcerative colitis (Jiang et al, 2018). Taken together, these studies support that the HSP90 isoforms exert different inflammatory effects; however, the findings were conflicting regarding the inhibition of which isoforms mediated anti-inflammatory effects. This indicates that the inflammatory role of HSP90 isoforms may vary depending on the cell type and disease context, highlighting the complex and heterogeneous effects of HSP90 inhibition on many client proteins and biological processes.

In this study, of the 4 HSP90 isoforms, only inhibition of TRAP1 exerted consistent anti-inflammatory effects. Numerous studies have evaluated the role of TRAP1 in cancer, suggesting that it is a key regulatory protein involved in many cellular pathways, although the literature on inflammatory effects is limited (Xie et al, 2020). In glioblastoma U251 cells, gamitrinib (a selective TRAP1 inhibitor) resulted in complete blockade of NF-κB activity after TNF stimulation, supporting our findings that TRAP1 inhibition may mediate anti-inflammatory effects (Siegelin et al, 2011). Given the pivotal role of keratinocytes in inflammatory skin diseases (Ben Abdallah et al, 2021; Jiang et al, 2020), TRAP1 inhibition may represent a promising therapeutic approach for topical treatment, warranting further investigation.

The pan-inhibitor RGRN-305 has been shown to exert strong anti-inflammatory effects in keratinocytes, which is

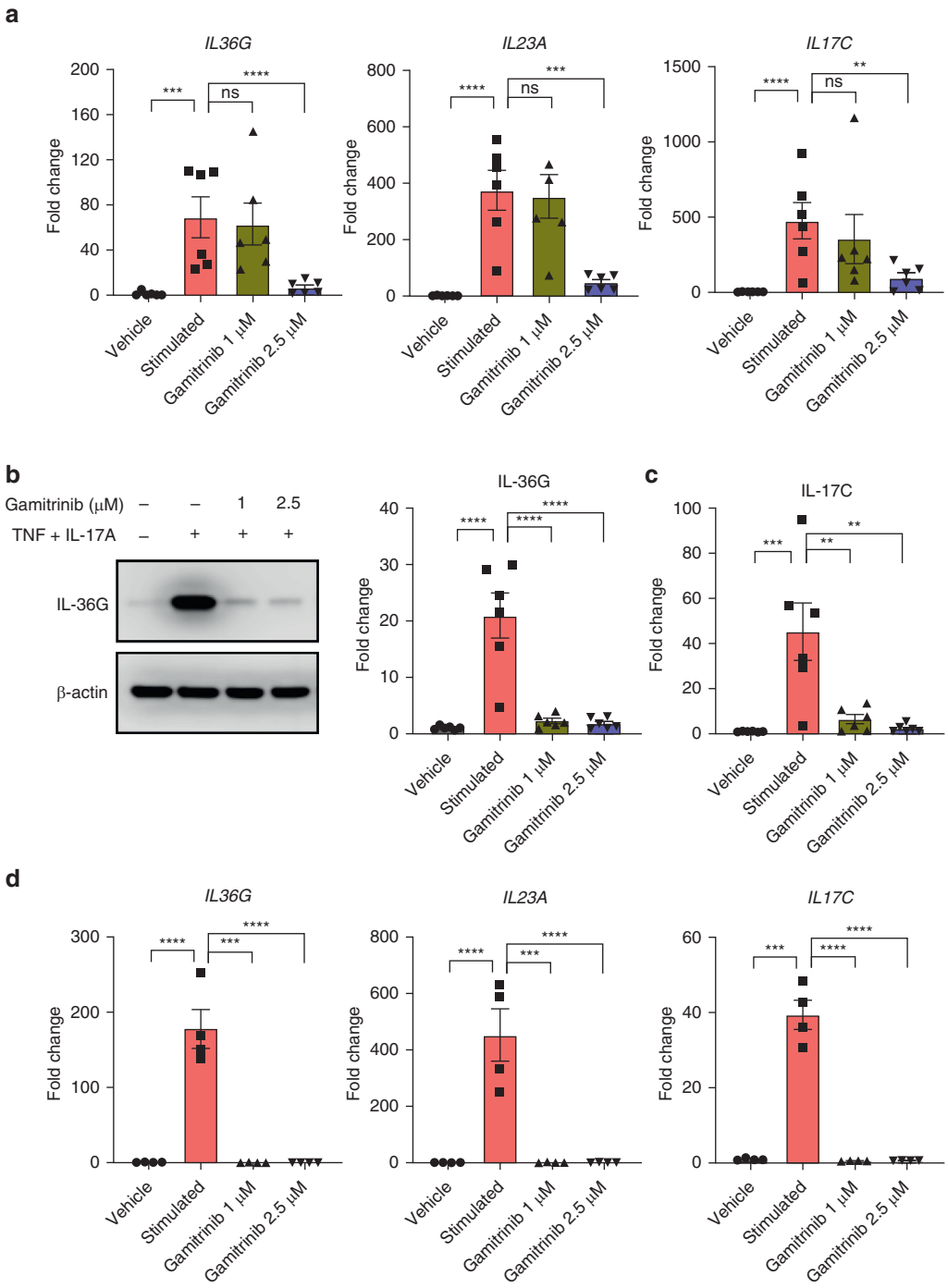

Figure 5. Effects of gamitrinib in keratinocytes and fibroblasts. Primary human keratinocytes were treated with gamitrinib (a selective TRAP1 inhibitor) and stimulated with TNF (10 ng/ml) and IL-17A (100 ng/ml) for 24 hours (3 independent experiments, n = 6). (**a**) Gene expression of *IL36G*, *IL23A*, and *IL17C* was measured with RT-qPCR. (**b**) Cell lysate IL-36G protein expression was determined by western blot, showing a representative image of a western blot (left) and densitometric results (right). (**c**) Cell supernatant IL-17C protein expression was quantified with ELISA. (**d**) The experiments with RT-qPCR analysis were also performed in primary human fibroblasts (n = 4). Data are shown as mean (+SEM) fold change relative to the vehicle group. *P*-values were calculated by paired ratio *t*-tests. $^{**}P \leq .01$, $^{***}P \leq .001$, and $^{****}P \leq .0001$. ns, not significant.

in contrast to the modest effect observed with siRNA knockdown of the 4 isoforms (Ben Abdallah et al, 2023a, 2023b; Hansen et al, 2021). This discrepancy may be due to off-target effects associated with small-molecule inhibitors or differences in the mode and extent of inhibition of HSP90 activity. For example, siRNA knockdown resulted in incomplete inhibition of HSP90 activity (ie, residual function), whereas HSP90 inhibitors usually only target the ATPase-dependant function, leaving nonchaperone functions unaffected. Furthermore, differences in compensatory mechanisms, such as the activation of the heat shock response, may also contribute to this discrepancy.

Our data suggest that the anti-inflammatory effects by TRAP1 knockdown may be counteracted by knockdown of the other isoforms in keratinocytes. The counteracting effects varied depending on the measured cytokine or chemokine. This variation could reflect differences in the molecular pathways regulating these inflammatory markers, or it may result from biologic and technical variability.

Limitations of this study include that siRNA-mediated knockdown of the HSP90 isoforms was only evaluated in

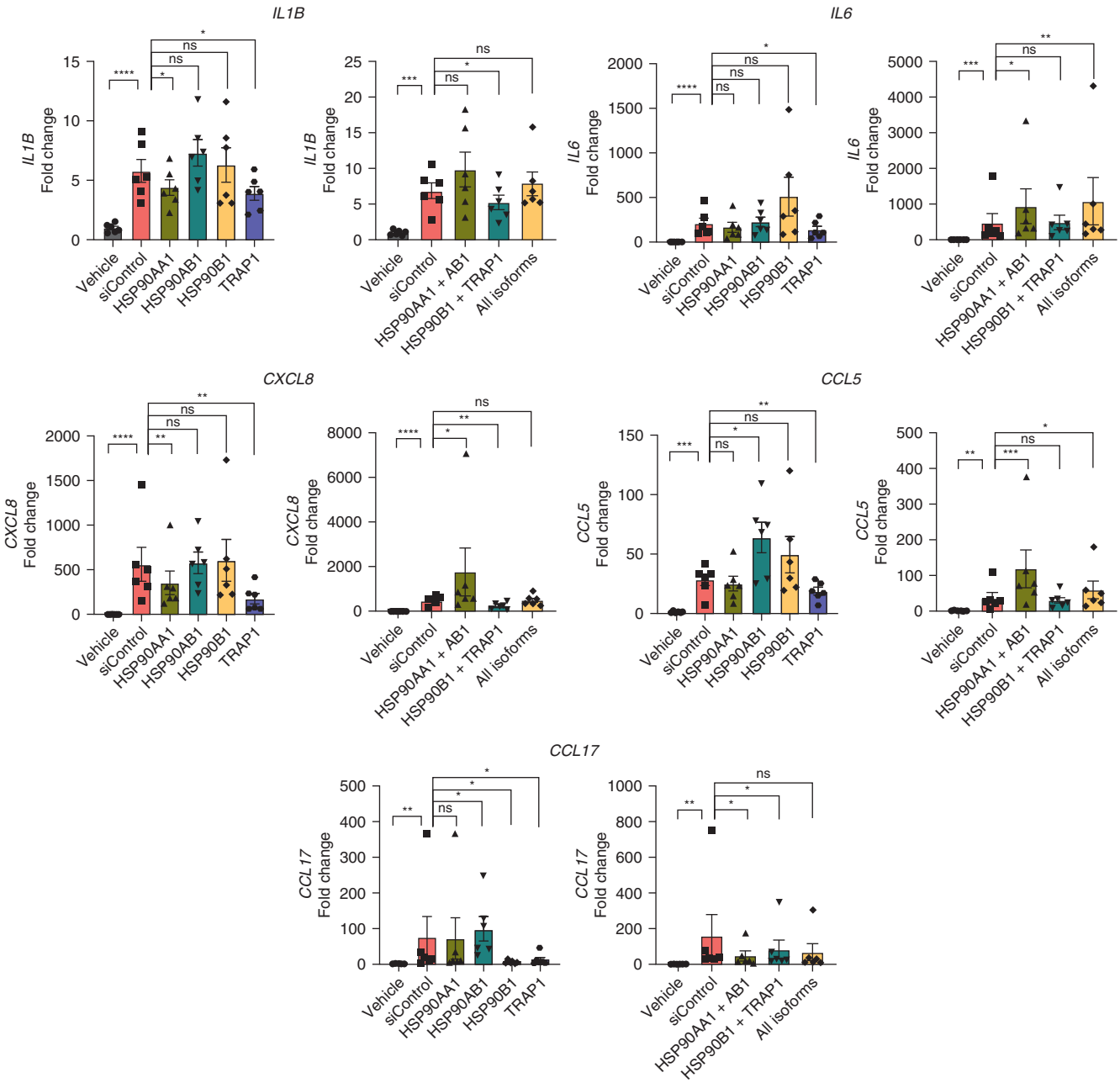

Figure 6. Effects of HSP90 isoform knockdown in atopic dermatitis–like stimulated keratinocytes. Selective and combined siRNA knockdown of the HSP90 isoforms was performed in primary human keratinocytes followed by stimulation with TNF (10 ng/ml), IL-4 (50 ng/ml), and IL-13 (50 ng/ml) for 24 hours (3 independent experiments, n = 6). Th1- and Th2-related gene expression was determined by RT-qPCR. Data are shown as mean (+SEM) fold change relative to the vehicle group. Wilcoxon rank-signed tests were used for statistical analysis of *CXCL8* and *CCL17*, whereas paired ratio *t*-tests were used for the other comparisons. $*P < .05$, $**P \leq .01$, $***P \leq .001$, and $****P \leq .0001$. ns, not significant; siRNA, small interfering RNA; Th1, T helper 1; Th2, T helper 2.

keratinocytes. However, the single-cell RNA analysis showed that *TRAP1* was mostly expressed in keratinocytes in the skin, indicating a predominant role in keratinocytes. In addition, TRAP1 inhibition with gamitrinib was evaluated in fibroblasts. Another limitation includes that these findings were not validated in a mouse model, which captures the biological complexity and contribution of different cell types in the skin. However, gamitrinib was evaluated in an ex vivo model with lesional hidradenitis suppurativa skin. Finally, the effects of HSP90 isoform inhibition on the transcriptome were not evaluated, which may have provided more comprehensive insights.

In conclusion, our findings demonstrate that selective and simultaneous inactivation of the HSP90 isoforms exert distinct anti-inflammatory effects. This highlights the importance of considering the isoform selectivity in the development of HSP90 inhibitors, which may impact the mechanism of action and the anti-inflammatory efficacy in treating inflammatory diseases. The drug distribution should also be considered because the expression and effects of the HSP90 isoforms may differ across various cell types and tissues. In addition, we discovered that selective TRAP1 inhibition exerted consistent anti-inflammatory effects, which may represent a therapeutic strategy. Further research is warranted

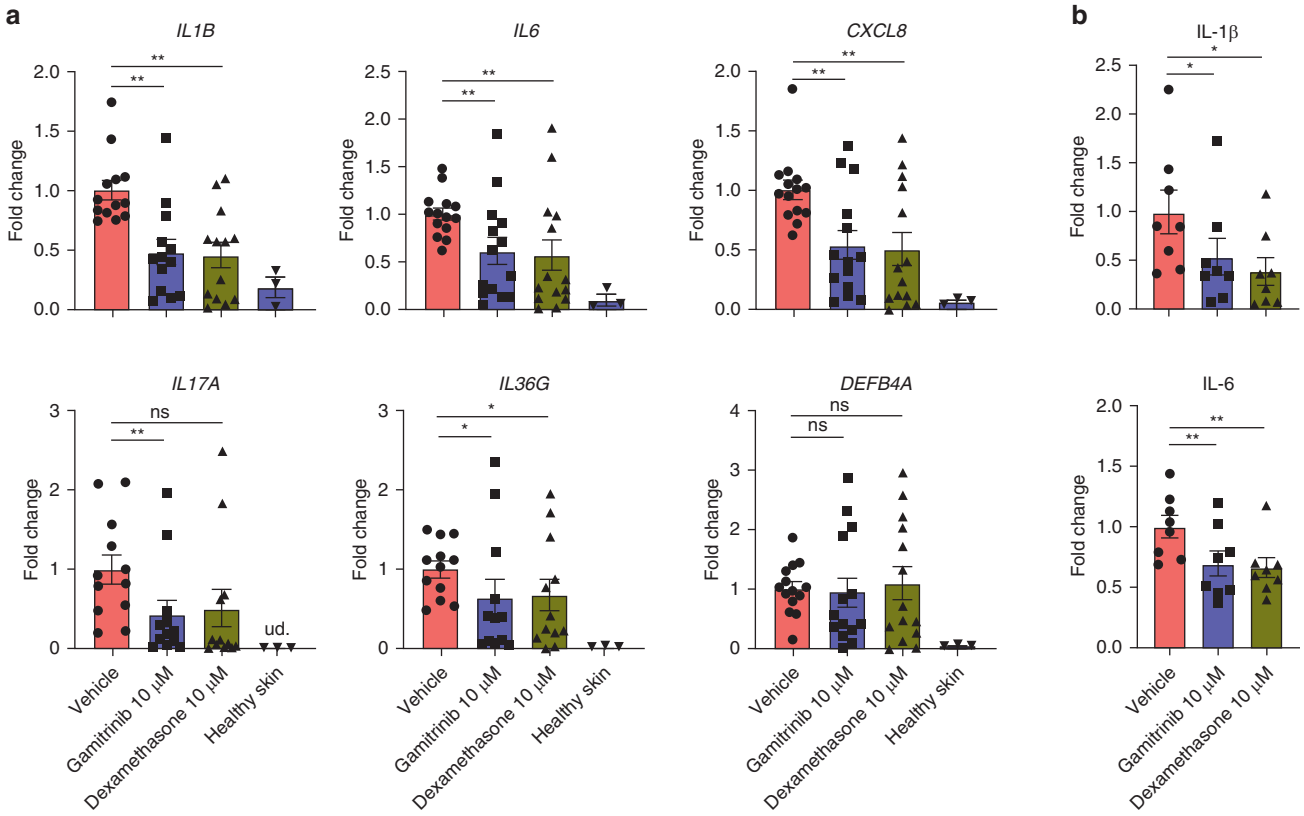

Figure 7. Effects of gamitrinib in an ex vivo model. Lesional hidradenitis suppurativa skin was treated ex vivo with vehicle (dimethyl sulfoxide), gamitrinib, or dexamethasone for 24 hours (n = 14). Healthy skin was only treated with vehicle (n = 3). (**a**) RT-qPCR and (**b**) ELISA were used to measure the gene and protein expression of indicated inflammatory genes, respectively. Data are shown as mean (+ SEM) fold change relative to that of the vehicle-treated lesional hidradenitis suppurativa skin. Wilcoxon rank-signed tests were used for statistical analysis of *IL17A* mRNA and IL-1β protein, whereas paired ratio *t*-tests were used for the other comparisons. $*P < .05$ and $**P \leq .01$. ud. denotes undetectable. ns, not significant.

to explore the effects of the HSP90 isoforms in inflammatory skin diseases, preferably in animal or small clinical studies, and to investigate the underlying molecular mechanisms of TRAP1 in inflammatory pathways.

MATERIALS AND METHODS

Cell culture and experiments

Primary normal human epidermal keratinocytes were isolated from 6 healthy donors as described previously (Johansen, 2017). Primary dermal fibroblasts were isolated from 4 healthy donors. The keratinocytes were cultured in keratinocyte SFM (Gibco, Thermo Fisher Scientific, Waltham, MA) supplemented with GFs and 5 μg/ml gentamicin (Gibco). The fibroblasts were cultured in DMEM supplemented with GlutaMAX (Gibco); 10% fetal bovine serum (Gibco); and antibiotics, including penicillin/streptomycin (10 μg/ml) and gentamycin (5 μg/ml). The cells were plated in 6-well plates and incubated at 37 °C in a humidified incubator containing 5% carbon dioxide until 60–70% confluency before the experiments were initiated.

Cell culture experiments with siRNA

The keratinocytes were transfected with DharmaFECT 2 (Dharmacon, Lafayette, CO) and ON-TARGETplus siRNA (Dharmacon) specific for *HSP90AA1* (catalog number 3320), *HSP90AB1* (number 3326), *HSP90B1* (number 7184), *TRAP1* (number 10131), or non-targeting control pool for 48 hours, following the manufacturer's instructions. The transfections were performed in 6-well plates in 2 ml medium with 50 nM siRNA for single-gene knockdown and 100 nM (total concentration) for multigene knockdown. After 48 hours of transfection, the medium was changed to basal medium (ie, without GFs) for 4 hours followed by stimulation with TNF (10 mg/ml, PeproTech, London, United Kingdom) + IL-17A (100 ng/ml, PeproTech) or TNF (10 ng/ml, PeproTech) + IL-4 (50 ng/ml, PeproTech) + IL-13 (50 ng/ml, PeproTech) for 24 hours to induce a phenotype mimicking psoriasis or atopic dermatitis.

Cell culture experiments with selective HSP90 inhibitors

The keratinocytes and fibroblasts were cultured in basal medium for 24 hours and preincubated with gamitrinib (TRAP1 inhibitor, HY-102007A, MedChemExpress, Monmouth Junction, NJ), TAS-116 (selective HSP90α/HSP90β inhibitor, HY-15785, MedChemExpress), or vehicle (dimethyl sulfoxide) for 4 hours followed by stimulation with IL-17A (100 ng/ml, PeproTech) or TNF (10 ng/ml, PeproTech) for 24 hours.

Ex vivo skin culture

A total of 3-mm punch biopsies were collected from excised skin with chronic hidradenitis suppurativa lesions from 14 patients and healthy skin from 3 donors. Immediately after collection, the biopsies were cultured in an ex vivo model as previously described (Companjen et al, 2001; Vossen et al, 2019). In summary, the biopsies were placed in 2-mm openings created in the membrane of Netwell Inserts (Corning, Corning, NY) with the epidermis in contact with air and dermis immersed in Iscove's Modified Dulbecco's Medium (Gibco) with 0.5% human male AB serum (Sigma-Aldrich,

Merck, Darmstadt, Germany) and streptomycin/penicillin (100 U/ml, Gibco). The biopsies were treated with vehicle (dimethyl sulfoxide), gamitrinib (10 μM, MedChemExpress), or dexamethasone (10 μM, Sigma-Aldrich) for 24 hours at 37 °C in a humidified incubator with 5% carbon dioxide.

RNA isolation

Total RNA was extracted from primary human keratinocytes and fibroblasts with the SV 96 Total RNA Isolation System (Promega, Madison, WI), following the manufacturer's instructions.

Punch biopsies were placed in RNAlater (Invitrogen, Thermo Fisher Scientific) and stored at 4 °C until further processing. The biopsies were added to SV RNA lysis buffer with β-mercaptoethanol (SV Total RNA Isolation System, Promega) followed by homogenization using TissueLyser (Qiagen, Hilden, Germany). The remaining steps, including RNA purification and DNase treatment, were conducted following the manufacturer's instructions.

NanoDrop 2000 Spectrophotometer (Thermo Fisher Scientific) was used to determine the RNA concentration and purity.

RT-qPCR

Total RNA was converted to cDNA using TaqMan Reverse Transcription Reagents, random hexamers (Thermo Fisher Scientific), and Peltier Thermal Cycler-200 (MJ Research, Waltham, MA) per the manufacturer's instructions. Real-time PCR was performed with StepOnePlus Real-Time PCR system (Themo Fisher Scientific) using 20 ng cDNA/reaction, TaqMan Universal PCR Master Mix, and primers/probes (Thermo Fisher Scientific) for *IL1B* (Hs01555410_m1), *IL6* (Hs00174131_m1), *IL17C* (Hs00171163_m1), *IL19* (Hs00604657_m1), *IL23A* (Hs00372324_m1), *IL36G* (Hs00219742_m1), *CXCL1* (Hs00236937_m1), *CCL5* (Hs00982282_m1), *CXCL8* (Hs00174103_m1), *CCL17* (Hs00171074_m1), *CCL20* (Hs00355476_m1), *NFKBIZ* (Hs00230071_m1), *HSP90AA1* (Hs00743767_sH), *HSP90AB1* (Hs03043878_g1), *HSP90B1* (Hs00427665_g1), *TRAP1* (Hs00212476_m1), *HSPA1A* (Hs00359163_s1), and *RPLP0* (Hs99999902_m1). Three technical replicates for each sample underwent real-time PCR, including 2 minutes at 50 °C and 10 minutes at 95 °C followed by 40 cycles of 15 seconds at 95 °C and 1 minute at 60 °C. The standard curve method and *RPLP0* (reference gene) were used to obtain normalized relative expression levels of target genes (Applied Biosystems, 2010).

Protein isolation from keratinocytes

Cell lysis buffer (cOmplete Protease Inhibitor Cocktail and phenylmethylsulphonyl fluoride [Sigma-Aldrich]) was added to primary human keratinocytes followed by centrifugation at 13,000*g* for 3 minutes. The protein extract was collected from the supernatant, and the protein concentration was determined by Bradford Protein Assay.

Western blot

Equal amounts of protein for each sample were loaded on 10% mini-PROTEAN TGX PreCast Gel (Bio-Rad Laboratories, Hercules, CA) and separated by gel electrophoresis using Mini Trans-Blot Cell (Bio-Rad Laboratories). The separated proteins were blotted onto nitrocellulose membranes with the Trans-Blot Turbo Transfer System (Bio-Rad Laboratories). The membranes were incubated overnight at 4 °C with the following primary antibodies: HSP90α (catalog number ab2928, Abcam, Cambridge, United Kingdom), HSP90β (catalog number ab53497, Abcam), GRP94 (catalog number ab2791, Abcam), TRAP1 (catalog number ab128914, Abcam), and IL-36G (catalog number AF2320, Bio-Techne, Minneapolis, MN). After washing, the membranes were incubated with horseradish peroxidase–conjugated secondary antibodies (catalog numbers P0447, P0448, P0449, or P0450, Dako, Glostrup, Denmark) at room temperature for 1 hour. Protein bands were visualized with Clarity Western ECL Substrate (Bio-Rad Laboratories) and C-DiGit Blot Scanner (LI-COR, Lincoln, NE). The protein expression was normalized to β-actin levels. The membranes were stripped and reprobed with an anti–β-actin antibody (A1978, Sigma-Aldrich), which was detected by horseradish peroxidase–conjugated anti-mouse IgG (catalog number P0447, Dako). Relative intensities of bands were quantified by densitometric analyses using Image Studio Digits, version 3.1 (LI-COR).

ELISA

The protein levels of IL-1β, IL-6, and IL-17C in culture medium were measured using commercial ELISA development kits (catalog numbers DY201, DY206, and DY1234, Bio-Techne) and a microplate spectrophotometer (Multiskan GO, Thermo Fisher Scientific) by following the manufacturer's instructions. All measurements were performed in duplicates.

Single-cell RNA-sequencing analysis

Single-cell RNA-sequencing datasets for psoriasis (GSE228421), hidradenitis suppurativa (GSE154775, GSE175990), atopic dermatitis (GSE222840), and healthy controls (GSE173205) were retrieved from the Gene Expression Omnibus. The R package Seurat (5.1.0) was used for the analysis (Hao et al, 2024). Cells with <200 or >6000 unique genes or >10% of mitochondrial gene expression were removed as low-quality cells. An integrative analysis of the datasets was performed following the workflow described in the Seurat vignette 'Integrative analysis in Seurat v5' using Anchor-based RPCA integration with default parameters (Satija, 2023). The findNeigbors and Findclusters function at a resolution of 0.4 was used to cluster the cells. Cell identities were annotated using published signature genes for the corresponding cell types (Francis et al, 2024; Franzén et al, 2019; Ma et al, 2023; van Straalen et al, 2024). The data were visualized using the DimPlot, Featureplot, VlnPlot, and Dotplot functions.

Immunohistochemistry

A total of 4-mm punch biopsies were fixed in 4% formaldehyde, paraffin embedded, and sliced into 4-μm sections for staining procedures. Heat-induced antigen retrieval was performed in citrate buffer (pH 6) for 20 minutes at preboiling temperature. The sections were incubated with anti-TRAP1 antibody (1:100, HPA044227, Atlas Antibodies, Stockholm, Sweden) for 1 hour at room temperature. The remaining steps of detection were performed using the Quanto Detection System (Thermo Fisher Scientific) per the manufacturer's instructions, followed by hematoxylin counterstaining. The slides were digitalized using the whole-slide scanner NanoZoomer 2.0-HT (Hamamatsu Photonics K.K, Hamamatsu City, Japan) with ×20 objective. Quantitative analysis of the images was performed using QuPath 0.4.2 and the Cell Detection command followed by a manual review with corrections (Bankhead et al, 2017). Isotype controls with normal rabbit IgG instead of TRAP1 antibody were performed and showed no staining.

Statistical analysis

Differences were analyzed with paired *t*-tests. If data were not normally distributed, Wilcoxon signed-rank tests were performed. $P <$

.05 was considered statistically significant. All analyses were performed in GraphPad Prism 10.0.3 or R software 4.3.2.

ETHICS STATEMENT

The experiments were approved by the Central Jutland Regional Committee on Health Research Ethics (M-20110027). The work described was performed in accordance with the Declaration of Helsinki. All donors were aged ≥18 years, and written informed consent was obtained from each donor.

DATA AVAILABILITY STATEMENT

The single-cell RNA-sequencing data are publicly available from Gene Expression Omnibus (GSE228421, https://www.ncbi.nlm.nih.gov/geo/query/acc.cgi?acc=GSE228421; GSE154775, https://www.ncbi.nlm.nih.gov/geo/query/acc.cgi?acc=GSE154775; GSE175990, https://www.ncbi.nlm.nih.gov/geo/query/acc.cgi?acc=GSE175990; GSE222840, https://www.ncbi.nlm.nih.gov/geo/query/acc.cgi?acc=GSE222840; and GSE173205, https://www.ncbi.nlm.nih.gov/geo/query/acc.cgi?acc=GSE173205). The data from RT-qPCR, western blot, ELISA, and immunohistochemistry are available from the corresponding author upon reasonable request.

ORCIDs

Hakim Ben Abdallah: http://orcid.org/0000-0002-4610-5428
Lars Iversen: http://orcid.org/0000-0003-1816-4508
Claus Johansen: http://orcid.org/0000-0002-5665-5212

CONFLICT OF INTEREST

LI has served as a consultant and/or paid speaker for and/or participated in clinical trials sponsored by AbbVie, Almirall, Amgen, Astra Zeneca, BMS, Boehringer Ingelheim, Celgene, Centocor, Eli Lilly, Janssen Cilag, Kyowa, Leo Pharma, MSD, Novartis, Pfizer, Regranion, Samsung, Union Therapeutics, and UCB. LI is also employed by MC2 Therapeutics A/S. CJ has served as a consultant and/or paid speaker for Eli Lilly, LEO Pharma, AbbVie, and L'Oréal. The remaining author states no conflict of interest.

ACKNOWLEDGMENTS

We thank Kongelig Hofbuntmager Aage Bangs Foundation for funding this study. We also thank Annette Blak Rasmussen, Kristine Møller, and Hang Pham Jensen for their technical assistance.

AUTHOR CONTRIBUTIONS

Conceptualization: HBA, LI, CJ; Formal Analysis: HBA, CJ; Funding Acquisition: HBA, LI, CJ; Methodology: HBA, LI, CJ; Project Administration: HBA, LI, CJ; Validation: HBA; Visualization: HBA; Supervision: LI, CJ; Writing — Original Draft Preparation: HBA, CJ; Writing — Review and Editing: HBA, LI, CJ

Disclaimer

The funder was not involved in the study design; collection, analysis, interpretation of data; preparation of manuscript, and/or publication decisions.

SUPPLEMENTARY MATERIAL

Supplementary material is linked to the online version of the paper at www.jidonline.org, and at https://doi.org/10.1016/j.jid.2025.02.006.

REFERENCES

Applied Biosystems. StepOne and StepOnePlus real-time PCR systems. https://assets.thermofisher.com/TFS-Assets/LSG/manuals/cms_046739.pdf; 2010 (accessed March 5, 2025).

Ausili A. Despite their structural similarities, the cytosolic isoforms of human Hsp90 show different behaviour in thermal unfolding due to their conformation: an FTIR study. Arch Biochem Biophys 2023;740:109599.

Bankhead P, Loughrey MB, Fernández JA, Dombrowski Y, McArt DG, Dunne PD, et al. QuPath: open source software for digital pathology image analysis. Sci Rep 2017;7:16878.

Ben Abdallah H, Bregnhøj A, Emmanuel T, Ghatnekar G, Johansen C, Iversen L. Efficacy and safety of the heat shock protein 90 inhibitor RGRN-305 in Hidradenitis Suppurativa: a parallel-design double-blind trial. JAMA Dermatol 2024;160:63–70.

Ben Abdallah H, Bregnhøj A, Ghatnekar G, Iversen L, Johansen C. Heat shock protein 90 inhibition attenuates inflammation in models of atopic dermatitis: a novel mechanism of action. Front Immunol 2023a;14:1289788.

Ben Abdallah H, Johansen C, Iversen L. Key signaling pathways in psoriasis: recent insights from antipsoriatic therapeutics. Psoriasis (Auckl) 2021;11:83–97.

Ben Abdallah H, Seeler S, Bregnhøj A, Ghatnekar G, Kristensen LS, Iversen L, et al. Heat shock protein 90 inhibitor RGRN-305 potently attenuates skin inflammation. Front Immunol 2023b;14:1128897.

Biebl MM, Buchner J. Structure, function, and regulation of the Hsp90 machinery. Cold Spring Harb Perspect Biol 2019;11:a034017.

Bregnhøj A, Thuesen KKH, Emmanuel T, Litman T, Grek CL, Ghatnekar GS, et al. HSP90 inhibitor RGRN-305 for oral treatment of plaque-type psoriasis: efficacy, safety and biomarker results in an open-label proof-of-concept study. Br J Dermatol 2022;186:861–74.

Companjen AR, van der Wel LI, Wei L, Laman JD, Prens EP. A modified ex vivo skin organ culture system for functional studies. Arch Dermatol Res 2001;293:184–90.

Costa TEMM, Raghavendra NM, Penido C. Natural heat shock protein 90 inhibitors in cancer and inflammation. Eur J Med Chem 2020;189:112063.

Echeverría PC, Bernthaler A, Dupuis P, Mayer B, Picard D. An interaction network predicted from public data as a discovery tool: application to the Hsp90 molecular chaperone machine. PLoS One 2011;6:e26044.

Francis L, McCluskey D, Ganier C, Jiang T, Du-Harpur X, Gabriel J, et al. Single-cell analysis of psoriasis resolution demonstrates an inflammatory fibroblast state targeted by IL-23 blockade. Nat Commun 2024;15:913.

Franzén O, Gan LM, Björkegren JLM. PanglaoDB: a web server for exploration of mouse and human single-cell RNA sequencing data. Database 2019 2019:baz046.

Hansen RS, Thuesen KKH, Bregnhøj A, Moldovan LI, Kristensen LS, Grek CL, et al. The HSP90 inhibitor RGRN-305 exhibits strong immunomodulatory effects in human keratinocytes. Exp Dermatol 2021;30:773–81.

Hao Y, Stuart T, Kowalski MH, et al. Dictionary learning for integrative, multimodal and scalable single-cell analysis. Nat Biotechnol 2024;42:293–304.

He GL, Luo Z, Shen TT, Yang J, Li P, Luo X, et al. Inhibition of HSP90β by ganetespib blocks the microglial signalling of evoked pro-inflammatory responses to heat shock. Int J Biochem Cell Biol 2019;106:35–45.

Hoy SM. Pimitespib: First approval. Drugs 2022;82:1413–8.

Jiang F, Guo AP, Xu JC, You QD, Xu XL. Discovery of a potent Grp94 selective inhibitor with anti-inflammatory efficacy in a mouse model of ulcerative colitis. J Med Chem 2018;61:9513–33.

Jiang Y, Tsoi LC, Billi AC, Ward NL, Harms PW, Zeng C, et al. Cytokinocytes: the diverse contribution of keratinocytes to immune responses in skin. JCI Insight 2020;5:e142067.

Johansen C. Generation and culturing of primary human keratinocytes from adult skin. J Vis Exp 2017;130:56863.

Li ZN, Luo Y. HSP90 inhibitors and cancer: prospects for use in targeted therapies (Review). Oncol Rep 2023;49:6.

Ma F, Plazyo O, Billi AC, Tsoi LC, Xing X, Wasikowski R, et al. Single cell and spatial sequencing define processes by which keratinocytes and fibroblasts amplify inflammatory responses in psoriasis. Nat Commun 2023;14:3455.

Maiti S, Picard D. Cytosolic Hsp90 isoform-specific functions and clinical significance. Biomolecules 2022;12:1166.

McClellan AJ, Tam S, Kaganovich D, Frydman J. Protein quality control: chaperones culling corrupt conformations. Nat Cell Biol 2005;7:736–41.

Miyata Y, Nakamoto H, Neckers L. The therapeutic target Hsp90 and cancer hallmarks. Curr Pharm Des 2013;19:347–65.

Nizami S, Arunasalam K, Green J, Cook J, Lawrence CB, Zarganes-Tzitzikas T, et al. Inhibition of the NLRP3 inflammasome by HSP90 inhibitors. Immunology 2021;162:84–91.

Park HK, Yoon NG, Lee JE, Hu S, Yoon S, Kim SY, et al. Unleashing the full potential of Hsp90 inhibitors as cancer therapeutics through simultaneous inactivation of Hsp90, Grp94, and TRAP1. Exp Mol Med 2020;52:79–91.

Picard D. Picard lab downloads. https://www.picard.ch/downloads/; 2023 (accessed January 4, 2024).

Satija R. Integrative analysis in Seurat v5. https://satijalab.org/seurat/articles/seurat5_integration; 2023 (accessed March 3, 2024).

Siegelin MD, Dohi T, Raskett CM, Orlowski GM, Powers CM, Gilbert CA, et al. Exploiting the mitochondrial unfolded protein response for cancer therapy in mice and human cells. J Clin Invest 2011;121:1349–60.

Smith AG, Kliebe VM, Mishra S, McCall RP, Irvine MM, Blagg BSJ, et al. Anti-inflammatory activities of novel heat shock protein 90 isoform selective inhibitors in BV-2 microglial cells. Front Mol Biosci 2024;11:1405339.

Stenderup K, Rosada C, Gavillet B, Vuagniaux G, Dam TN. Debio 0932, a new oral Hsp90 inhibitor, alleviates psoriasis in a xenograft transplantation model. Acta Derm Venereol 2014;94:672–6.

Taipale M, Jarosz DF, Lindquist S. HSP90 at the hub of protein homeostasis: emerging mechanistic insights. Nat Rev Mol Cell Biol 2010;11:515–28.

Trepel J, Mollapour M, Giaccone G, Neckers L. Targeting the dynamic HSP90 complex in cancer. Nat Rev Cancer 2010;10:537–49.

Tukaj S, Bieber K, Kleszczyński K, Witte M, Cames R, Kalies K, et al. Topically applied Hsp90 Blocker 17AAG inhibits autoantibody-mediated blister-inducing cutaneous inflammation. J Invest Dermatol 2017;137:341–9.

Tukaj S, Tiburzy B, Manz R, de Castro Marques A, Orosz A, Ludwig RJ, et al. Immunomodulatory effects of heat shock protein 90 inhibition on humoral immune responses. Exp Dermatol 2014;23:585–90.

van Straalen KR, Ma F, Tsou PS, Plazyo O, Gharaee-Kermani M, Calbet M, et al. Single-cell sequencing reveals Hippo signaling as a driver of fibrosis in hidradenitis suppurativa. J Clin Invest 2024;134:e169225.

Vossen ARJV, Ardon CB, van der Zee HH, Lubberts E, Prens EP. The anti-inflammatory potency of biologics targeting tumour necrosis factor-α, interleukin (IL)-17A, IL-12/23 and CD20 in hidradenitis suppurativa: an ex vivo study. Br J Dermatol 2019;181:314–23.

Wang C, Wu L, Bulek K, Martin BN, Zepp JA, Kang Z, et al. The psoriasis-associated D10N variant of the adaptor Act1 with impaired regulation by the molecular chaperone hsp90. Nat Immunol 2013;14:72–81.

Xie S, Wang X, Gan S, Tang X, Kang X, Zhu S. The mitochondrial chaperone TRAP1 as a candidate target of oncotherapy. Front Oncol 2020;10:585047.

Yu J, Zhang C, Song C. Pan- and isoform-specific inhibition of Hsp90: design strategy and recent advances. Eur J Med Chem 2022;238:114516.

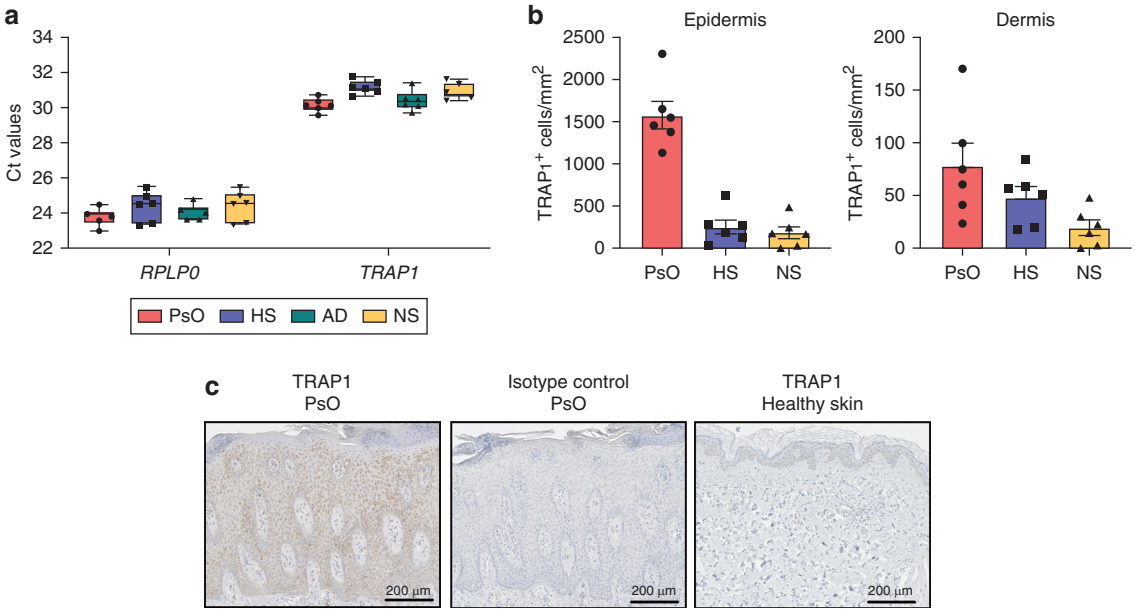

Supplementary Figure S1. The expression of the HSP90 isoforms in the skin. (**a**) The RT-qPCR cycle threshold (Ct) values for *TRAP1* and *RPLP0* in PsO (n = 6), HS (n = 6), AD (n = 6), and normal (n = 6) skin. Data are shown as box plots with whiskers ranging from the minimum to the maximum data point. (**b**) Quantitative immunohistochemical analysis of $TRAP1^+$ cells in PsO (n = 6), HS (n = 6), and normal (n = 6) skin. Results are shown as mean (+SEM) of $TRAP^+$ cells per mm^2 of epidermis or dermis. (**c**) Representative images of $TRAP1^+$ stained sections from psoriatic skin, healthy skin, and isotype control staining. AD, atopic dermatitis; HS, hidradenitis suppurativa; NS, normal skin; PsO, psoriasis.

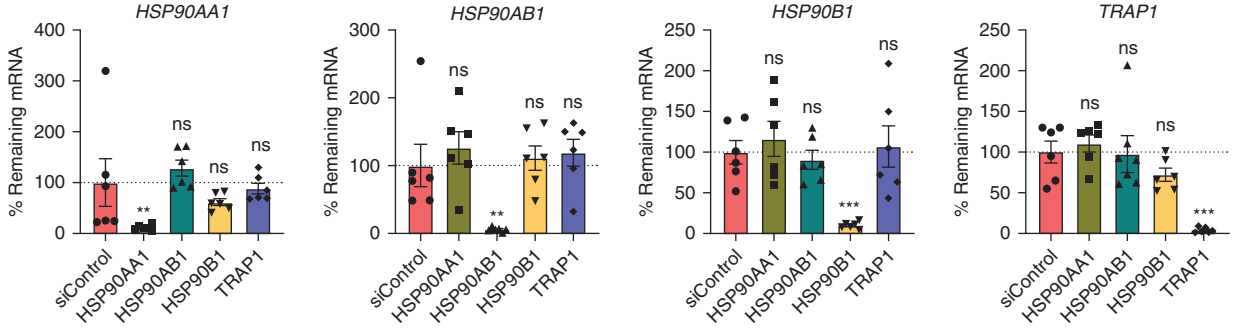

Supplementary Figure S2. Knockdown efficiency and specificity on mRNA level. RT-qPCR analysis of the remaining gene expression of the HSP90 isoforms in keratinocytes transfected with siRNA for 48 hours followed by TNF + IL-17A stimulation for 24 hours (n = 6). The data are shown as mean (+SEM) fold change relative to that of keratinocytes treated with a nontargeting siRNA control pool (siControl). *P*-values were calculated by paired ratio *t*-tests. $^{**}P \leq .01$ and $^{***}P \leq .001$. ns, not significant; siControl, control-targeted small interfering RNA; siRNA, small interfering RNA.

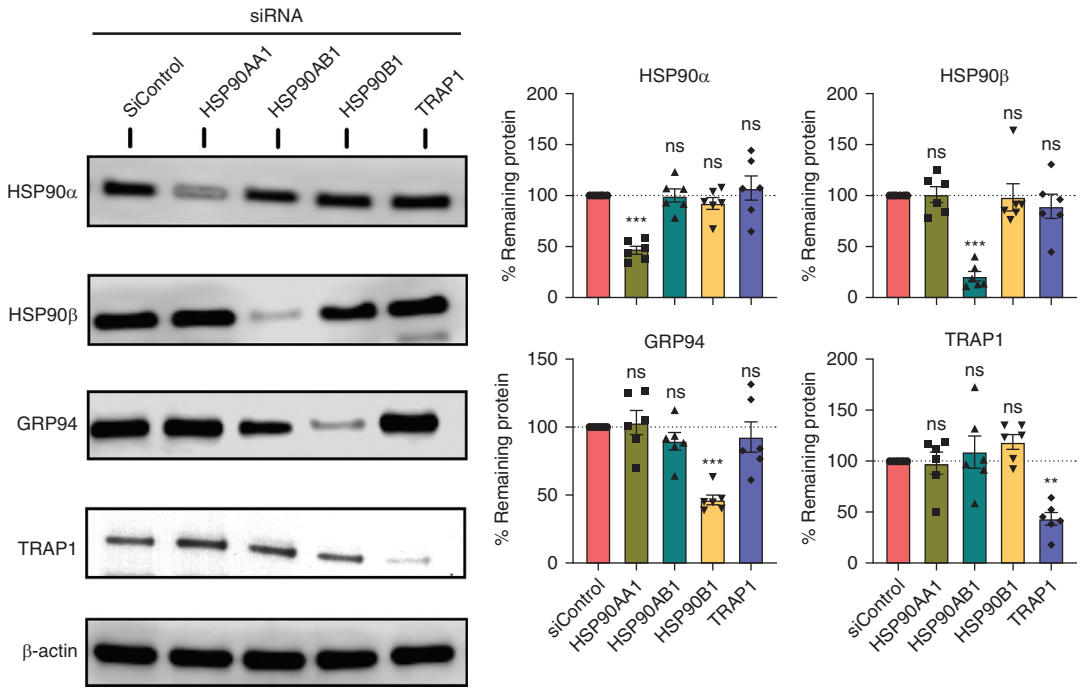

Supplementary Figure S3. Knockdown efficiency and specificity on protein level. The remaining protein expression of the HSP90 isoforms was determined by western blot in keratinocytes transfected with siRNA for 48 hours followed by TNF (10 ng/ml) + IL-17A (100 ng/ml) stimulation for 24 hours (n = 6). Representative western blots and densitometric results (mean + SEM) are shown. *P*-values were calculated by paired ratio *t*-tests. $^{**}P \leq .01$ and $^{***}P \leq .001$. ns, not significant; siRNA, small interfering RNA.

Supplementary Figure S4. *HSPA1A* gene expression. The gene expression of *HSPA1A* (encoding HSP70 protein) was measured by RT-qPCR in keratinocytes (**a**) transfected with siRNA targeting the HSP90 isoforms or (**b**) treated with gamitrinib (a selective TRAP1 inhibitor) or TAS-116 (a selective HSP90α/β inhibitor). *P*-values were calculated by paired ratio *t*-tests. $^{*}P < .05$, $^{**}P \leq .01$, and $^{****}P \leq .0001$. ns, not significant; siControl, control-targeted small interfering RNA; siRNA, small interfering RNA.

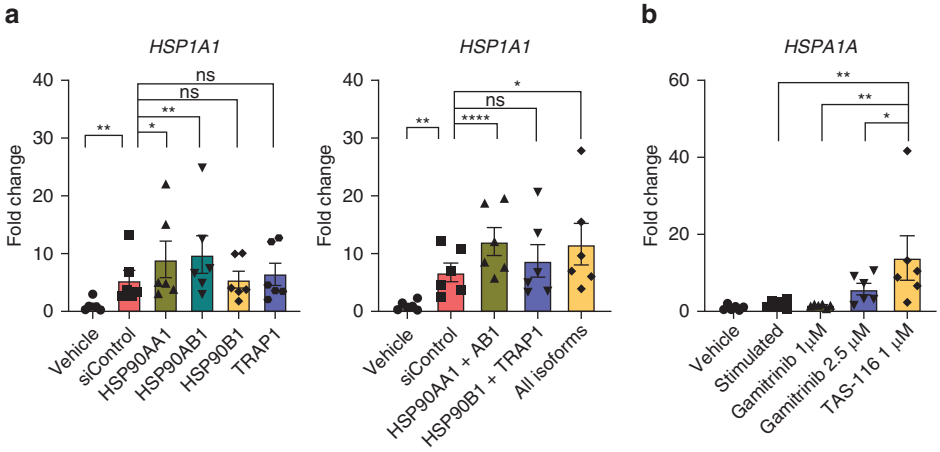

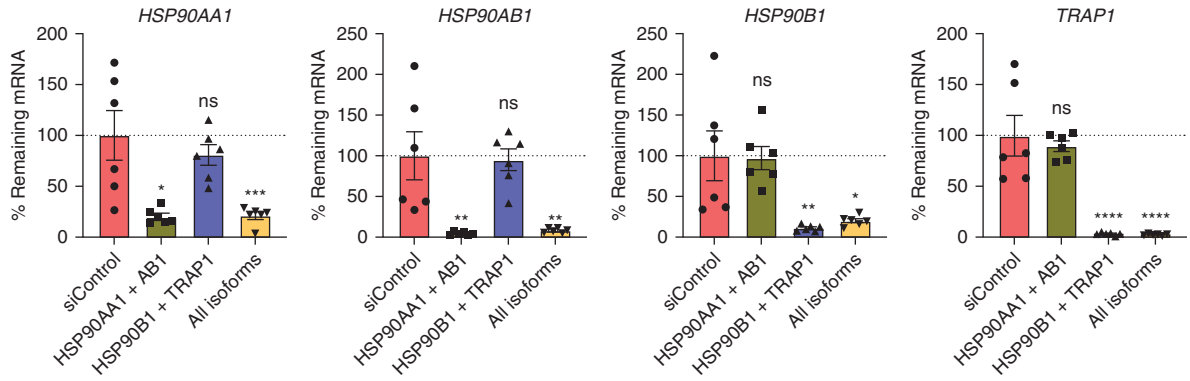

Supplementary Figure S5. Efficiency and specificity of combined HSP90 isoform knockdown. Shown is the remaining gene expression of the HSP90 isoforms in keratinocytes after combined siRNA transfection for 48 hours and then stimulation with TNF (10 ng/ml) + IL-17A (100 ng/ml) for 24 hours (n = 6). The RT-qPCR data are shown as mean (+SEM) fold change relative to that of keratinocytes transfected with a nontargeting siRNA control pool (siControl). *P*-values were calculated by paired ratio *t*-tests. $*P < .05$, $**P \leq .01$, $***P \leq .001$, and $****P \leq .0001$. ns, not significant; siControl, control-targeted small interfering RNA; siRNA, small interfering RNA.